Published in final edited form as:
Ultrasound Obstet Gynecol. 2011 April ; 37(4): 423–431. doi:10.1002/uog.8840.

FAST (Four chamber view And Swing Technique) Echo: a Novel and Simple Algorithm to Visualize Standard Fetal Echocardiographic Planes

Lami Yeo, MD[1,2], **Roberto Romero, MD**[1,2,3], **Cristiano Jodicke, MD**[1,2], **Giovanna Oggè, MD**[1], **Wesley Lee, MD**[1,2,4], **Juan Pedro Kusanovic, MD**[1,2], **Edi Vaisbuch, MD**[1,2], and **Sonia S. Hassan, MD**[1,2]

[1] Perinatology Research Branch, NICHD/NIH/DHHS, Bethesda, Maryland, and Detroit, Michigan, USA

[2] Department of Obstetrics and Gynecology, Wayne State University, Detroit, Michigan, USA

[3] Center for Molecular Medicine and Genetics, Wayne State University, Detroit, Michigan, USA

[4] Division of Fetal Imaging, Department of Obstetrics and Gynecology, William Beaumont Hospital, Royal Oak, Michigan, USA

Abstract

Objective—To describe a novel and simple algorithm (FAST Echo: Four chamber view And Swing Technique) to visualize standard diagnostic planes of fetal echocardiography from dataset volumes obtained with spatiotemporal image correlation (STIC) and applying a new display technology (OmniView).

Methods—We developed an algorithm to image standard fetal echocardiographic planes by drawing four dissecting lines through the longitudinal view of the ductal arch contained in a STIC volume dataset. Three of the lines are locked to provide simultaneous visualization of targeted planes, and the fourth line (unlocked) "swings" through the ductal arch image ("swing technique"), providing an infinite number of cardiac planes in sequence. Each line generated the following plane(s): 1) Line 1: three-vessels and trachea view; 2) Line 2: five-chamber view and long axis view of the aorta (obtained by rotation of the five-chamber view on the y-axis); 3) Line 3: four-chamber view; and 4) "Swing" line: three-vessels and trachea view, five-chamber view and/or long axis view of the aorta, four-chamber view, and stomach. The algorithm was then tested in 50 normal hearts (15.3 – 40 weeks of gestation) and visualization rates for cardiac diagnostic planes were calculated. To determine if the algorithm could identify planes that departed from the normal images, we tested the algorithm in 5 cases with proven congenital heart defects.

Results—In normal cases, the FAST Echo algorithm (3 locked lines and rotation of the five-chamber view on the y-axis) was able to generate the intended planes (longitudinal view of the ductal arch, pulmonary artery, three-vessels and trachea view, five-chamber view, long axis view of the aorta, four-chamber view): 1) individually in 100% of cases [except for the three-vessel and trachea view, which was seen in 98% (49/50)]; and 2) simultaneously in 98% (49/50). The "swing technique" was able to generate the three-vessels and trachea view, five-chamber view and/or long

Address correspondence to: Lami Yeo, M.D. and Roberto Romero, M.D., Perinatology Research Branch, NICHD, NIH, DHHS, Wayne State University/Hutzel Women's Hospital, 3990 John R, Box 4, Detroit, MI 48201, USA, Telephone (313) 993–2700, Fax: (313) 993–2694, Lami Yeo: lyeo@med.wayne.edu, Roberto Romero: prbchiefstaff@med.wayne.edu.

*R. Romero has contributed to this work as part of his official duties as employee of the United States Federal Government.

NIH-PA Author Manuscript
NIH-PA Author Manuscript

axis view of the aorta, four-chamber view, and stomach in 100% of normal cases. In the abnormal cases, the FAST Echo algorithm demonstrated the cardiac defects and displayed views that deviated from what was expected from the examination of normal hearts. The "swing technique" was useful in demonstrating the specific diagnosis due to visualization of an infinite number of cardiac planes in sequence.

Conclusions—This novel and simple algorithm can be used to visualize standard fetal echocardiographic planes in normal fetal hearts. The FAST Echo algorithm may simplify examination of the fetal heart and could reduce operator dependency. Using this algorithm, the inability to obtain expected views or the appearance of abnormal views in the generated planes should raise the index of suspicion for congenital heart disease.

Keywords

STIC; prenatal diagnosis; congenital heart disease; ultrasound; four-dimensional; fetal heart

Introduction

Congenital heart disease has a prevalence of 8 per 1000 live births,[1] and is a major cause of infant and childhood mortality.[2] However, only 6–35% of congenital heart defects are identified prenatally.[3–15] Indeed, recent evidence indicates that despite almost universal access to sonographic screening during pregnancy, only 28% of major congenital heart defects were detected prenatally.[16] Anatomical defects of the fetal heart remain difficult to diagnose due to the complex structure of the organ and the high degree of expertise required for a thorough examination.[17–19] Prenatal detection of major forms of congenital heart disease may improve preoperative conditions,[20–24] survival after surgery,[22,25–27] and neurologic outcomes.[28] Therefore, the development of algorithms to facilitate examination of the fetal heart could increase the detection rates of congenital heart disease and reduce associated perinatal morbidity and mortality.

Two-dimensional sonography of the fetal heart relies on obtaining standard anatomic planes, including the four-chamber view, left and right outflow tracts, and three-vessels and trachea view.29–34 However, successfully obtaining these views is highly dependent on operator skills and experience. A solid body of evidence35[–61] indicates that three-dimensional (3D) and four-dimensional ultrasonography (4DUS) with spatiotemporal image correlation (STIC) can facilitate visualization of standard cardiac diagnostic planes, reducing operator dependency. Four-dimensional STIC technology allows the acquisition of a volume dataset from the fetal heart, and displays a cine loop of a complete single cardiac cycle in motion. OmniView (GE Medical Systems, Kretztechnik GmbH, Zipf, Austria) is a new display technology for 3D and 4DUS which allows interrogation of volume datasets and the simultaneous display of up to three independent (non-orthogonal) planes by manually drawing straight or curved lines from any direction or angle. This is in contrast to tomographic ultrasound imaging (TUI), which allows volume datasets to be automatically sliced, displaying multiple parallel images to each other. However, the lines which produce these slices are rigid, equidistant from each other, and cannot be rotated or drawn manually.

We describe herein a novel and simple algorithm (using STIC and OmniView) to visualize the standard diagnostic planes of fetal echocardiography: the FAST (Four-chamber view And Swing Technique) Echo. The potential diagnostic value of the FAST Echo algorithm is also illustrated in five cases of congenital heart defects.

Methods

Using STIC technology (Voluson 730 Expert, Voluson E8 Expert; GE Medical Systems, Kretztechnik GmbH, Zipf, Austria), 4D volume datasets of the fetal heart were acquired from an apical four-chamber view with hybrid mechanical and curved array transducers (2–5 or 4–8 MHz) by transverse sweeps through the fetal chest in patients examined at our unit. Acquisition time ranged from 7.5 to 15 seconds, and the angle of acquisition ranged between 20° and 40°, depending on fetal motion and gestational age. All patients had been enrolled in research protocols approved by the Institutional Review Board of the National Institute of Child Health and Human Development and by the Human Investigation Committee of Wayne State University. All women had provided written informed consent for the use of ultrasound images for research purposes.

Volume datasets considered by the investigators to be of adequate quality were selected: 1) the fetal spine was positioned between the 5- and 7-o'clock positions, minimizing the possibility of shadowing from the ribs or spine; and 2) minimal or no motion artifacts were observed on the sagittal plane. Volume datasets that did not contain the upper mediastinum were excluded. Only one volume dataset per patient was included in the study.

From normal fetal hearts, a standardized algorithm was developed for the analysis of volume datasets to obtain the standard diagnostic planes of fetal echocardiography. This was accomplished by retrospectively reviewing datasets off-line using 4D View (Version 9.1.1.0) (GE Healthcare, Waukesha, WI, USA) and applying OmniView technology. The algorithm was then tested in 50 normal hearts (15.3 – 40 weeks of gestation). OmniView allows interrogation of volume datasets (3D or 4D) and the simultaneous display of up to three independent (non-orthogonal) planes by manually drawing straight or curved lines from any direction or angle. The lines which can be selected are: "line", "curve", "polyline", and "trace". Once the drawn line is completed, it may be rotated or moved through any part of the image. Therefore, using OmniView to dissect volume datasets has the following features: 1) multiple independent planes can be generated which are not necessarily parallel to each other; 2) the planes can be targeted to display the anatomical areas of interest; 3) informative views are easier to obtain than other methods involving complex manipulation of volume datasets, and the informative planes are visualized immediately; 4) "virtual" planes can be generated which cannot be obtained by using TUI or the standard multiplanar display because curvilinear planes can be imaged; 5) images may be displayed as a plane, or in conjunction with Volume Contrast Imaging (VCI) (GE Medical Systems, Kretztechnik, Zipf, Austria), an application of 3D ultrasound that displays a thin slice from an acquired volume where the slice thickness can be adjusted to improve contrast resolution; and 6) through VCI, images can be viewed from either side of the section plane.

Representative volumes from normal fetuses at 26, 28, and 30 weeks of gestation were used to illustrate the FAST echo algorithm for this communication. Additionally, the algorithm was applied to volume datasets from 5 fetuses with congenital heart defects (confirmed postnatally by echocardiography, surgery, or during autopsy): tricuspid atresia with ventricular septal defect (hypoplastic right ventricle) (21 weeks of gestation), tetralogy of Fallot (33 weeks of gestation), complete atrioventricular canal defect/transposition of the great vessels (30 weeks of gestation), transposition of the great vessels with normal four-chamber view (20 weeks of gestation), and hypoplastic left heart/double outlet right ventricle/transposition of great vessels/heterotaxy (19 weeks of gestation).

Results

Description of FAST Echo Algorithm

The acronym "FAST" represents the acquisition of all STIC volume datasets from the four-chamber view, the "swing technique", and also refers to the performance speed of the algorithm. The algorithm consists of drawing four dissecting lines through the longitudinal view of the ductal arch image; three of the lines are locked to provide simultaneous visualization of targeted planes, and the fourth line (unlocked) "swings" through the ductal arch image ("swing technique"), providing an infinite number of cardiac planes in sequence. Using this algorithm, the following planes are visualized: 1) longitudinal view of the ductal arch; 2) pulmonary artery; 3) three-vessels and trachea view; 4) five-chamber view; 5) long axis view of the aorta; 6) four-chamber view; and 7) stomach.

All STIC volume datasets were displayed using the multiplanar modality, which demonstrates three orthogonal planes (panels A, B, and C). The FAST Echo algorithm was performed in the following steps:

1. Volume datasets are adjusted to display the apical four-chamber view in panel A, where the cross-section of the aorta is aligned with the crux of the heart (6 o'clock) (Figure 1). The left ventricle is always oriented towards the left side of the image.
2. The reference dot is positioned in the lumen of the aorta, and this allows visualization of a coronal view of the descending aorta in panel C (Figure 1). The image is rotated in panel C so that the aorta is imaged in a vertical or semi-vertical position in order to visualize the longitudinal view of the ductal arch in panel B (Figure 2). The next step is to place the reference dot in the crux of the heart (panel A) (Figure 3).
3. The speed of the STIC cine-loop is then decreased to 50% to facilitate drawing of the independent lines and visualization of the diagnostic planes when using the "swing technique." The longitudinal view of the ductal arch image in panel B (Figure 3) is selected, and the OmniView option is activated. Three independent lines (Lines 1, 2, 3) are drawn through the ductal arch image from the top to the bottom of the image, and then locked into place, so that the "lollipop" is oriented downwards. Each of the lines is activated by clicking first on their respective button in 4D View. To ensure that the "lollipop" is oriented downwards, the arrowhead pointing to the *right* (located in the "Orientation" panel of 4D View) should be clicked. At the starting point of each of the lines, the mouse should be clicked only once and *released*, and a cursor will appear at the inferior end of the line. This allows the operator to visualize the line as it is being drawn, as well as the corresponding image simultaneously. Lines are locked by clicking the mouse again, and the cursor will become a "lollipop." Once lines are locked, they can be rotated or moved through any part of the image. The end result is that each drawn line will generate various cardiac diagnostic planes. The following is a step-by-step description of the images generated by each line:
    a. <u>Three-vessels and trachea view</u>: Line 1 (yellow) is a diagonal line drawn through the center of the pulmonary artery parallel to and equidistant from the walls, until it reaches the level of the descending aorta or below (Figure 4). Once Line 1 is completed, it is locked into place by clicking the mouse. The pulmonary artery, aorta, superior vena cava, and trachea will be visualized (Figure 4, A).
    b. <u>Five-chamber view</u>: Line 2 (fuchsia) is a vertical line (6 o'clock) drawn through the right ventricle, center of the aorta (cross-section), left atrium,

and descending aorta (Figure 4). Once Line 2 is completed, it is locked into place by clicking the mouse. The five-chamber view (both atria, both ventricles, aortic root) will be visualized (Figure 4, B).

c. Four-chamber view: Line 3 (turquoise) is a vertical line (6 o'clock) drawn through the right ventricle, right external edge of the aorta (cross-section), left atrium, and descending aorta (Figure 4). Once Line 3 is completed, it is locked into place by clicking the mouse. The four-chamber view will be visualized (Figure 4, C).

4. When the three lines are completed, the three-vessels and trachea view, five-chamber view, and four-chamber view will be simultaneously visualized (along with the original longitudinal view of the ductal arch/pulmonary artery) (Figure 4) as a continuous cine-loop (Videos 1, 2).

5. Long axis view of the aorta: The Rotation Y option is selected by clicking on the bar, and the five-chamber view is rotated by scrolling on the y-axis (to the right) until the long axis view of the aorta is visualized (Figure 5). Next, a scroll on the y-axis (back to the left) is performed until the original views (three-vessels and trachea view, five-chamber view, four-chamber view) are again simultaneously visualized. The next step will be performance of the "swing technique."

6. Swing technique: Any of the 3 Lines (yellow, fuchsia, turquoise) may function as the "swing" line, and is a matter of preference. At the top of the longitudinal view of the ductal arch image, the "swing" line is begun approximately above the center of the right ventricle and is *fixed (but not locked)* on this end only, by clicking the mouse once and releasing. The line is then drawn from the top to the lower left hand corner of the image, making sure it is lateral to the ductal arch (Figure 6); however, it should remain *unlocked* with the cursor (not the "lollipop") visualized at its inferior end. The line is then swung like a pendulum *unlocked* throughout the entire image from the left to the right side, ending at the lower right hand corner of the image (Video 3). The "swing" line may also be moved in the opposite direction (right to left) throughout the ductal arch image. As a result, the "swing technique" generates an infinite number of cardiac planes in sequence. The planes having diagnostic value[62] (reported in sequence here from left to right) are: three-vessels and trachea view, long axis view of the aorta, five-chamber view, four-chamber view, and stomach. It is noteworthy that by keeping the line *unlocked*, the pivot point will remain at the superior end of the line, and provide a wide field of view with undistorted images. However, once the line is *locked*, the pivot point will move to the center of the line, and with line rotation, the images may appear unrecognizable and non-informative.

7. Once the FAST Echo algorithm is completed, the cardiac views visualized as a continuous cine-loop include: longitudinal view of the ductal arch, pulmonary artery, three-vessels and trachea view, five-chamber view, long axis view of the aorta, four-chamber view, and stomach. Video 4 demonstrates the entire FAST Echo algorithm.

8. Depending on the image quality, VCI can be activated with a slice thickness of 2 mm (Figure 7 and Video 5). This allows images to appear smoother and the interface between different tissues to be more apparent.

Visualization Rates for Echocardiographic Planes in Normal Fetuses

The FAST Echo algorithm (3 locked lines and rotation of the five-chamber view on the y-axis) was able to generate the intended planes (longitudinal view of the ductal arch,

NIH-PA Author Manuscript

NIH-PA Author Manuscript

pulmonary artery, three-vessels and trachea view, five-chamber view, long axis view of the aorta, four-chamber view): 1) individually in 100% of cases [except for the three-vessels and trachea view, which was seen in 98% (49/50)]; and 2) simultaneously in 98% (49/50). The "swing technique" was able to generate the three-vessels and trachea view, five-chamber view and/or long axis view of the aorta, four-chamber view, and stomach in 100% of normal cases. In one case where the three-vessels and trachea view was not seen using the 3 locked lines, the "swing technique" was able to generate this plane. Moreover, in 24% (12/50) of cases, the "swing technique" was able to generate the long axis view of the aorta; therefore, rotation of the five-chamber view on the y-axis to generate this view was not mandatory. For the 76% (38/50) of cases where the "swing technique" depicted the five-chamber view (but not the long axis view of the aorta), rotation of the five-chamber view on the y-axis to generate this view was required.

FAST Echo Algorithm Applied to Five Cases of Congenital Heart Disease

Tricuspid atresia with ventricular septal defect (hypoplastic right ventricle)— The FAST Echo algorithm is illustrated in a fetus with tricuspid atresia and ventricular septal defect (hypoplastic right ventricle) at 21 weeks of gestation (Figure 8 and Video 6). The longitudinal view of the ductal arch appears abnormal, and both this view and the three-vessels and trachea view (Line 1) show a small pulmonary artery, consistent with pulmonic stenosis. Placement of Line 2 shows the aorta arising from the left ventricle and this is also evident with rotation of the five-chamber view on the y-axis. The four-chamber view is abnormal (Line 3), with a large ventricular septal defect, and a hypoplastic right ventricle. The tricuspid valve is atretic, while the mitral valve moves normally.

Tetralogy of Fallot—Figure 9 and Video 7 show a fetus with tetralogy of Fallot at 33 weeks of gestation. Placement of Line 1 shows evidence of pulmonic stenosis with an abnormally thickened valve with poor motility, while placement of Line 2 shows the overriding aorta. Placement of Line 3 shows an abnormal four-chamber view with a large ventricular septal defect.

Complete atrioventricular canal defect, transposition of great vessels—The FAST Echo algorithm is illustrated in a fetus with complete atrioventricular canal defect and transposition of the great vessels at 30 weeks of gestation (Figure 10 and Video 8). In the longitudinal view of the ductal arch, the descending aorta is visualized, but not the pulmonary artery. The three-vessels and trachea view (Line 1) is abnormal, and shows the aorta, superior vena cava, and trachea; however, the pulmonary artery is not visualized. In the five-chamber view (Line 2), the aorta is visualized anteriorly, while the pulmonary artery (confirmed by its bifurcation) arises leftward from the common ventricular chamber. The four-chamber view (Line 3) shows a common atrioventricular valve and a large septal defect involving both the atrial and ventricular septa.

Transposition of great vessels with the appearance of a normal four-chamber view—In this fetus with transposition of the great vessels at 20 weeks of gestation (Figure 11, Video 9), the four-chamber view appears normal (Line 3). However, in the longitudinal view of the ductal arch, the pulmonary artery and ductus arteriosus are not visualized. The three-vessels and trachea view (Line 1) is abnormal, and shows only the aorta (arising from the right ventricle) and superior vena cava. After placement of Line 2, the pulmonary artery (confirmed by its bifurcation) is seen exiting the left ventricle; with rotation of this image on the y-axis, the aorta is visualized arising anteriorly from the right ventricle (also shown by the "swing technique").

Hypoplastic left heart, double outlet right ventricle, transposition of great vessels, heterotaxy—The FAST Echo algorithm is illustrated in a fetus at 19 weeks of gestation with a complex cardiac defect (Figure 12 and Video 10). In the longitudinal view of the ductal arch, the descending aorta is visualized, but the pulmonary artery and ductus arteriosus are not seen. The three-vessels and trachea view (Line 1) is abnormal, and shows the aorta arising from the right ventricle. After placement of Line 2, the pulmonary artery (confirmed by its bifurcation) is seen to exit leftwards from the right ventricle. The four-chamber view (Line 3) shows the hypoplastic left heart. The "swing technique" demonstrates the congenital heart defect by depicting: 1) two great vessels exiting only the right ventricle which are also transposed (pulmonary artery leftwards, aorta rightwards and anterior); and 2) the stomach on the fetal right side.

Swing Technique

The addition of the novel "swing technique" offers several advantages to that of only drawing 3 locked lines through the longitudinal view of the ductal arch image and rotating the five-chamber view on the y-axis: 1) the stomach can be visualized, provided that the angle of acquisition of the STIC volume is adequate; 2) the three-vessels and trachea view was generated only by the "swing technique" (n=1); 3) in 24% (12/50) of cases, the "swing technique" was able to generate the long axis view of the aorta, and therefore, rotation of the five-chamber view on the y-axis to generate this view was not mandatory; and 4) an infinite number of cardiac planes are generated *in sequence*, and therefore, was found to be useful in demonstrating congenital heart defects. Moreover, by using the "swing" line: 1) the operator can freely move the line back and forth in any direction or angle, and at any speed throughout the longitudinal view of the ductal arch image according to one's preference; and 2) when navigating with the "swing" line, the user may lock this line at any time (once the desired image is generated) so that the image can be studied, or stored/printed for the medical record.

Discussion

In a 1980 seminal study correlating sonographic planes used in fetal echocardiography to anatomic sections of the thorax in aborted fetuses (12–28 weeks of gestation), Allan et al. reported that the sonographic plane most easily obtained in the fetus was the four-chamber view of the heart.[63] Subsequently, the four-chamber view was introduced as a screening tool for the prenatal detection of congenital heart disease.[64,65] It still remains the primary screening method,[66–70] and has been included as part of the fetal cardiac examination by regulatory organizations.[19,71–73] Due to this fact, the FAST Echo algorithm was developed based upon the acquisition of all STIC volume datasets from the four-chamber view.

The use of 4D STIC to evaluate the fetal heart is advantageous because it allows the user to navigate within the cardiac volume dataset, obtain all of the standard image planes necessary for diagnosis, and reduces operator dependency.[44] However, retrieving informative diagnostic planes from a volume dataset that contains infinite planes is difficult. Moreover, many operators examine the fetal heart without using a systematic approach. Therefore, algorithms have been developed to systematically examine 3D/4D volume datasets, so that diagnostic planes can be displayed in an efficient manner.[45,74,75] Others have developed a system for the automated display of such planes from a volume dataset of the fetal heart.[76]

We report herein a novel and simple algorithm to visualize standard fetal echocardiographic planes from dataset volumes obtained with STIC and applying OmniView technology. Indeed, five "short axis views," including the three-vessels and trachea view, have been proposed as a screening method for comprehensive fetal echocardiography.[62] These sonographic planes can easily be obtained by reslicing volume datasets of the fetal heart obtained with STIC, as shown by the FAST Echo algorithm. In abnormal cases, the algorithm demonstrated the cardiac defects and displayed views that deviated from what was expected from the examination of normal hearts. Moreover, the "swing technique" was useful in demonstrating the specific diagnosis in abnormal cases, due to visualization of cardiac planes in sequence by moving the "swing" line through the volume dataset. This concept has been described by Professor Lindsay Allan, who reported the technique of performing fetal echocardiography and obtaining transverse views of the heart.[29] With the fetus in a long-axis projection, the ultrasound beam can be swept in a horizontal plane from the stomach upwards to image the four-chamber view, the aortic outflow tract, the pulmonary outflow tract, and the transverse view of the aortic arch in sequence. Professor Allan described that by using a manual approach, a small change in the transducer angle can produce all of these cardiac views, and will usually demonstrate all the features necessary to define a normal heart.[29]

It is important to stress that the FAST Echo algorithm will not be successful if: 1) the quality of the STIC volume dataset is inadequate; 2) the volume dataset does not contain information about the cardiac diagnostic planes; and 3) a true four-chamber view is not depicted in panel A (e.g. true cross-section of the thorax, proper alignment in the axial plane, etc.). Therefore, proper acquisition of STIC volume datasets is essential to perform the algorithm. The algorithm may also be applied to a 3D static acquisition; however, this is not the optimal approach and there are potential important limitations: 1) valvular motion and color Doppler sonography cannot be assessed; and 2) because of cardiac motion, a static acquisition will combine the information of different phases of the cardiac cycle, which may result in artifact and poor resolution/definition of key anatomic structures required for diagnosis (e.g. valves may appear blurred). Thus, by applying our algorithm to 3D static acquisitions, the success rate of visualizing standard fetal echocardiographic planes may be affected. Moreover, using STIC volume datasets allows the operator to select the part of the cardiac cycle where interrogation is to be undertaken, thus optimizing image quality (e.g. peak-systole will result in a well-defined image of the outflow tracts). This is the optimal method of examination of normal and abnormal fetal hearts.

The introduction of new display techniques, such as the one proposed herein, may simplify examination of the fetal heart and could reduce operator dependency. Even if one operator acquires the STIC volume dataset, it is possible for another operator to apply the FAST Echo algorithm to the dataset. Moreover, we found that the algorithm improved understanding of the 3D anatomy of the fetal heart, and therefore may be useful as a teaching tool. Using the FAST Echo algorithm, the inability to obtain expected views or the appearance of abnormal views in the generated planes should raise the index of suspicion for congenital heart disease. Studies to test the reproducibility and agreement of this algorithm are in progress.

Acknowledgments

This research was supported by the Perinatology Research Branch, Division of Intramural Research, *Eunice Kennedy Shriver* National Institute of Child Health and Human Development, NIH, DHHS.

References

1. Montana E, Khoury MJ, Cragan JD, Sharma S, Dhar P, Fyfe D. Trends and outcomes after prenatal diagnosis of congenital cardiac malformations by fetal echocardiography in a well defined birth population, Atlanta Georgia. 1990–1994. J Am Coll Cardiol. 1996; 28:1805–1809. [PubMed: 8962570]

2. Boneva RS, Botto LD, Moore CA, Yang Q, Correa A, Erickson JD. Mortality associated with congenital heart defects in the United States: trends and racial disparities, 1979–1997. Circulation. 2001; 103:2376–2381. [PubMed: 11352887]
3. Montana E, Khoury MJ, Cragan JD, Sharma S, Dhar P, Fyfe D. Trends and outcomes after prenatal diagnosis of congenital cardiac malformations by fetal echocardiography in a well defined birth population, Atlanta Georgia. 1990–1994. J Am Coll Cardiol. 1996; 28:1805–1809. [PubMed: 8962570]
4. Cooper MJ, Enderlein MA, Dyson DC, Roge CL, Tarnoff H. Fetal echocardiography: retrospective review of clinical experience and an evaluation of indications. Obstet Gynecol. 1995; 86:577–582. [PubMed: 7675383]
5. Stoll C, Alembik Y, Dott B, Roth PM, De Geeter B. Evaluation of prenatal diagnosis of congenital heart disease. Prenat Diagn. 1993; 13:453–461. [PubMed: 8372071]
6. Crane JP, LeFevre ML, Winborn RC, Evans JK, Ewigman BG, Bain RP, Frigoletto FD, McNellis D. A randomized trial of prenatal ultrasonographic screening: impact on the detection, management, and outcome of anomalous fetuses. The RADIUS Study Group. Am J Obstet Gynecol. 1994; 171:392–399. [PubMed: 8059817]
7. Rustico MA, Benettoni A, D'Ottavio G, Maieron A, Fischer-Tamaro I, Conoscenti G, Meir Y, Montesano M, Cattaneo A, Mandruzzato G. Fetal heart screening in low-risk pregnancies. Ultrasound Obstet Gynecol. 1995; 6:313–319. [PubMed: 8590200]
8. Buskens E, Grobbee DE, Frohn-Mulder IME, Stewart PA, Juttmann RE, Wladimiroff JW, Hess J. Efficacy of routine fetal ultrasound screening for congenital heart disease in normal pregnancy. Circulation. 1996; 94:67–72. [PubMed: 8964120]
9. Todros T, Faggiano F, Chiappa E, Gaglioti P, Mitola B, Sciarrone A. Accuracy of routine ultrasonography in screening heart disease prenatally. Gruppo Piemontese for Prenatal Screening of Congenital Heart Disease. Prenat Diagn. 1997; 17:901–906. [PubMed: 9358568]
10. Fernandez CO, Ramaciotti C, Martin LB, Twickler DM. The four-chamber view and its sensitivity in detecting congenital heart defects. Cardiology. 1998; 90:202–206. [PubMed: 9892769]
11. Stoll C, Alembik Y, Dott B, Meyer MJ, Pennerath A, Peter MO, DeGeeter B. Evaluation of prenatal diagnosis of congenital heart disease. Prenat Diagn. 1998; 18:801–807. [PubMed: 9742567]
12. Grandjean H, Larroque D, Levi S. The performance of routine ultrasonographic screening of pregnancies in the Eurofetus Study. Am J Obstet Gynecol. 1999; 181:446–454. [PubMed: 10454699]
13. Klein SK, Cans C, Robert E, Jouk PS. Efficacy of routine fetal ultrasound screening for congenital heart disease in Isere County, France. Prenat Diagn. 1999; 19:318–322. [PubMed: 10327135]
14. Garne E, Stoll C, Clementi M. Evaluation of prenatal diagnosis of congenital heart diseases by ultrasound: experience from 20 European registries. Ultrasound Obstet Gynecol. 2001; 17:386–391. [PubMed: 11380961]
15. Jaeggi ET, Sholler GF, Jones OD, Cooper SG. Comparative analysis of pattern, management and outcome of pre- versus postnatally diagnosed major congenital heart disease: a population-based study. Ultrasound Obstet Gynecol. 2001; 17:380–385. [PubMed: 11380960]
16. Friedberg MK, Silverman NH, Moon-Grady AJ, Tong E, Nourse J, Sorenson B, Lee J, Hornberger LK. Prenatal detection of congenital heart disease. J Pediatr. 2009; 155:26–31. [PubMed: 19394031]
17. Hunter S, Heads A, Wyllie J, Robson S. Prenatal diagnosis of congenital heart disease in the northern region of England: benefits of a training programme for obstetric ultrasonographers. Heart. 2000; 84:294–298. [PubMed: 10956294]
18. Tegnander E, Eik-Nes SH. The examiner's ultrasound experience has a significant impact on the detection rate of congenital heart defects at the second-trimester fetal examination. Ultrasound Obstet Gynecol. 2004; 24:217. [PubMed: 15329970]
19. International Society of Ultrasound in Obstetrics and Gynecology Guidelines. Cardiac screening examination of the fetus: guidelines for performing the "basic" and "extended basic" cardiac scans. Ultrasound Obstet Gynecol. 2006; 27:107–113. [PubMed: 16374757]

20. Schultz AH, Localio AR, Clark BJ, Ravishankar C, Videon N, Kimmel SE. Epidemiologic features of the presentation of critical congenital heart disease: implications for screening. Pediatrics. 2008; 121:751–757. [PubMed: 18381540]

21. Brown KL, Ridout DA, Hoskote A, Verhulst L, Ricci M, Bull C. Delayed diagnosis of congenital heart disease worsens preoperative condition and outcome of surgery in neonates. Heart. 2006; 92:1298–1302. [PubMed: 16449514]

22. Tworetzky W, McElhinney DB, Reddy VM, Brook MM, Hanley FL, Silverman NH. Improved surgical outcome after fetal diagnosis of hypoplastic left heart syndrome. Circulation. 2001; 103:1269–1273. [PubMed: 11238272]

23. Verheijen PM, Lisowski LA, Stoutenbeek P, Hitchcock JF, Bennink GK, Meijboom EJ. Lactacidosis in the neonate is minimized by prenatal detection of congenital heart disease. Ultrasound Obstet Gynecol. 2002; 19:552–555. [PubMed: 12047532]

24. Kumar RK, Newburger JW, Gauvreau K, Kamenir SA, Hornberger LK. Comparison of outcome when hypoplastic left heart syndrome and transposition of the great arteries are diagnosed prenatally versus when diagnosis of these two conditions is made only postnatally. Am J Cardiol. 1999; 83:1649–1653. [PubMed: 10392870]

25. Bonnet D, Coltri A, Butera G, Fermont L, Le Bidois J, Kachaner J, Sidi D. Detection of transposition of the great arteries in fetuses reduces neonatal morbidity and mortality. Circulation. 1999; 99:916–918. [PubMed: 10027815]

26. Khoshnood B, De Vigan C, Vodovar V, Goujard J, Lhomme A, Bonnet D, Goffinet F. Trends in prenatal diagnosis, pregnancy termination, and perinatal mortality of newborns with congenital heart disease in France, 1983–2000: a population-based evaluation. Pediatrics. 2005; 115:95–101. [PubMed: 15629987]

27. Franklin O, Burch M, Manning N, Sleeman K, Gould S, Archer N. Prenatal diagnosis of coarctation of the aorta improves survival and reduces morbidity. Heart. 2002; 87:67–69. [PubMed: 11751670]

28. Mahle WT, Clancy RR, McGaurn SP, Goin JE, Clark BJ. Impact of prenatal diagnosis on survival and early neurologic morbidity in neonates with the hypoplastic left heart syndrome. Pediatrics. 2001; 107:1277–1282. [PubMed: 11389243]

29. Allan L. Technique of fetal echocardiography. Pediatr Cardiol. 2004; 25:223–233. [PubMed: 15360115]

30. Benacerraf BR. Sonographic detection of fetal anomalies of the aortic and pulmonary arteries: value of four-chamber view vs. direct images. AJR Am J Roentgenol. 1994; 163:1483–1489. [PubMed: 7992752]

31. Carvalho JS, Mavrides E, Shinebourne EA, Campbell S, Thilaganathan B. Improving the effectiveness of routine prenatal screening for major congenital heart defects. Heart. 2002; 88:387–391. [PubMed: 12231598]

32. Chaoui, R. The examination of the normal fetal heart using two-dimensional fetal echocardiography. In: Yagel, S.; Silverman, NH.; Gembruch, U., editors. Fetal Cardiology. Martin Dunitz; London: 2003. p. 141-149.

33. Bromley B, Estroff JA, Sanders SP, Parad R, Roberts D, Frigoletto FD Jr, Benacerraf BR. Fetal echocardiography: accuracy and limitations in a population at high and low risk for heart defects. Am J Obstet Gynecol. 1992; 166:1473–1481. [PubMed: 1595802]

34. Comstock CH. What to expect from routine midtrimester screening for congenital heart disease. Semin Perinatol. 2000; 24:331–342. [PubMed: 11071374]

35. Bennasar M, Martínez JM, Olivella A, del Río M, Gómez O, Figueras F, Puerto B, Gratacós E. Feasibility and accuracy of fetal echocardiography using four-dimensional spatiotemporal image correlation technology before 16 weeks' gestation. Ultrasound Obstet Gynecol. 2009; 33:645–651. [PubMed: 19479815]

36. Nelson TR, Pretorius DH, Sklansky M, Hagen-Ansert S. Three-dimensional echocardiographic evaluation of fetal heart anatomy and function: acquisition, analysis, and display. J Ultrasound Med. 1996; 15:1–9. [PubMed: 8667477]

37. Turan S, Turan OM, Ty-Torredes K, Harman CR, Baschat AA. Standardization of the first-trimester fetal cardiac examination using spatiotemporal image correlation with tomographic

ultrasound and color Doppler imaging. Ultrasound Obstet Gynecol. 2009; 33:652–656. [PubMed: 19405042]

38. Nelson TR. Three-dimensional fetal echocardiography. Prog Biophys Mol Biol. 1998; 69:257–272. [PubMed: 9785942]
39. Paladini D, Sglavo G, Greco E, Nappi C. Cardiac screening by STIC: can sonologists performing the 20-week anomaly scan pick up outflow tract abnormalities by scrolling the A-plane of STIC volumes? Ultrasound Obstet Gynecol. 2008; 32:865–870. [PubMed: 19035539]
40. Sklansky MS, Nelson T, Strachan M, Pretorius DH. Real-time three-dimensional fetal echocardiography: initial feasibility study. J Ultrasound Med. 1999; 18:745–752. [PubMed: 10547106]
41. Shih JC, Shyu MK, Su YN, Chiang YC, Lin CH, Lee CN. ‘Big-eyed frog’ sign on spatiotemporal image correlation (STIC) in the antenatal diagnosis of transposition of the great arteries. Ultrasound Obstet Gynecol. 2008; 32:762–768. [PubMed: 18780310]
42. Bega G, Kuhlman K, Lev-Toaff A, Kurtz A, Wapner R. Application of three-dimensional ultrasonography in the evaluation of the fetal heart. J Ultrasound Med. 2001; 20:307–313. [PubMed: 11316308]
43. Uittenbogaard LB, Haak MC, Spreeuwenberg MD, Van Vugt JM. A systematic analysis of the feasibility of four-dimensional ultrasound imaging using spatiotemporal image correlation in routine fetal echocardiography. Ultrasound Obstet Gynecol. 2008; 31:625–632. [PubMed: 18504769]
44. DeVore GR, Falkensammer P, Sklansky MS, Platt LD. Spatio-temporal image correlation (STIC): new technology for evaluation of the fetal heart. Ultrasound Obstet Gynecol. 2003; 22:380–387. [PubMed: 14528474]
45. Gonçalves LF, Lee W, Chaiworapongsa T, Espinoza J, Schoen ML, Falkensammer P, Treadwell M, Romero R. Four-dimensional ultrasonography of the fetal heart with spatiotemporal image correlation. Am J Obstet Gynecol. 2003; 189:1792–1802. [PubMed: 14710117]
46. Jurgens J, Chaoui R. Three-dimensional multiplanar time-motion ultrasound or anatomical M-mode of the fetal heart: a new technique in fetal echocardiography. Ultrasound Obstet Gynecol. 2003; 21:119–123. [PubMed: 12601830]
47. Maulik D, Nanda NC, Singh V, Dod H, Vengala S, Sinha A, Sidhu MS, Khanna D, Lysikiewicz A, Sicuranza G, Modh N. Live three-dimensional echocardiography of the human fetus. Echocardiography. 2003; 20:715–721. [PubMed: 14641376]
48. Vinals F, Poblete P, Giuliano A. Spatio-temporal image correlation (STIC): a new tool for the prenatal screening of congenital heart defects. Ultrasound Obstet Gynecol. 2003; 22:388–394. [PubMed: 14528475]
49. Abuhamad A. Automated multiplanar imaging: a novel approach to ultrasonography. J Ultrasound Med. 2004; 23:573–576. [PubMed: 15154522]
50. Chaoui R, Hoffmann J, Heling KS. Three-dimensional (3D) and 4D color Doppler fetal echocardiography using spatiotemporal image correlation (STIC). Ultrasound Obstet Gynecol. 2004; 23:535–545. [PubMed: 15170792]
51. Espinoza J, Gonçalves LF, Lee W, Chaiworapongsa T, Treadwell MC, Stites S, Schoen ML, Mazor M, Romero R. The use of the minimum projection mode in 4-dimensional examination of the fetal heart with spatiotemporal image correlation. J Ultrasound Med. 2004; 23:1337–1348. [PubMed: 15448324]
52. Gonçalves LF, Espinoza J, Lee W, Mazor M, Romero R. Three- and four-dimensional reconstruction of the aortic and ductal arches using inversion mode: a new rendering algorithm for visualization of fluid-filled anatomical structures. Ultrasound Obstet Gynecol. 2004; 24:696–698. [PubMed: 15521086]
53. Gonçalves LF, Espinoza J, Romero R, et al. A systematic approach to prenatal diagnosis of transposition of the great arteries using 4-dimensional ultrasonography with spatiotemporal image correlation. J Ultrasound Med. 2004; 23:1225–1231. [PubMed: 15328439]
54. Gonçalves LF, Romero R, Espinoza J, Lee W, Treadwell M, Chintala K, Brandl H, Chaiworapongsa T. Four-dimensional ultrasonography of the fetal heart using color Doppler spatiotemporal image correlation. J Ultrasound Med. 2004; 23:473–481. [PubMed: 15098864]

55. Viñals F, Ascenzo R, Naveas R, Huggon I, Giuliano A. Fetal echocardiography at 11 + 0 to 13 + 6 weeks using four-dimensional spatiotemporal image correlation telemedicine via an Internet link: a pilot study. Ultrasound Obstet Gynecol. 2008; 31:633–638. [PubMed: 18461551]
56. Espinoza J, Gonçalves LF, Lee W, Mazor M, Romero R. A novel method to improve prenatal diagnosis of abnormal systemic venous connections using three-and four-dimensional ultrasonography and "inversion mode. Ultrasound Obstet Gynecol. 2005; 25:428–434. [PubMed: 15846761]
57. Gonçalves LF, Espinoza J, Lee W, Nien JK, Hong JS, Santolaya-Forgas J, Mazor M, Romero R. A new approach to fetal echocardiography: digital casts of the fetal cardiac chambers and great vessels for detection of congenital heart disease. J Ultrasound Med. 2005; 24:415–424. [PubMed: 15784759]
58. Gindes L, Hegesh J, Weisz B, Gilboa Y, Achiron R. Three and four dimensional ultrasound: a novel method for evaluating fetal cardiac anomalies. Prenat Diagn. 2009; 29:645–653. [PubMed: 19340842]
59. Yagel S, Cohen SM, Shapiro I, Valsky DV. 3D and 4D ultrasound in fetal cardiac scanning: a new look at the fetal heart. Ultrasound Obstet Gynecol. 2007; 29:81–95. [PubMed: 17200988]
60. Gonçalves LF, Espinoza J, Romero R, Kusanovic JP, Swope B, Nien JK, Erez O, Soto E, Treadwell MC. Four-dimensional ultrasonography of the fetal heart using a novel Tomographic Ultrasound Imaging display. J Perinat Med. 2006; 34:39–55. [PubMed: 16489885]
61. Chaoui R, Heling KS. New developments in fetal heart scanning: three- and four-dimensional fetal echocardiography. Semin Fetal Neonatal Med. 2005; 10:567–577. [PubMed: 16242390]
62. Yagel S, Cohen SM, Achiron R. Examination of the fetal heart by five short-axis views: a proposed screening method for comprehensive cardiac evaluation. Ultrasound Obstet Gynecol. 2001; 17:367–369. [PubMed: 11380958]
63. Allan LD, Tynan MJ, Campbell S, Wilkinson JL, Anderson RH. Echocardiographic and anatomical correlates in the fetus. Br Heart J. 1980; 44:444–451. [PubMed: 7426207]
64. DeVore GR. The prenatal diagnosis of congenital heart disease: a practical approach for the fetal sonographer. J Clin Ultrasound. 1985; 13:229–245. [PubMed: 3923046]
65. Allan LD, Crawford DC, Chita SK, Tynan MJ. Prenatal screening for congenital heart disease. BMJ. 1986; 292:1717–1719. [PubMed: 3089369]
66. Sharland GK, Allan LD. Screening for congenital heart disease prenatally. Results of a 2 1/2-year study in the South East Thames Region. Br J Obstet Gynaecol. 1992; 99:220–225. [PubMed: 1606121]
67. Stephens JD. Accuracy of apical four-chamber view as screen for congenital heart disease. Am J Obstet Gynecol. 1990; 163:249–250. [PubMed: 2197868]
68. Gembruch U, Knopfle G, Chatterjee M, Bald R, Redel DA, Födisch HJ, Hansmann M. Prenatal diagnosis of atrioventricular canal malformations with up-to-date echocardiographic technology: report of 14 cases. Am Heart J. 1991; 121:1489–1497. [PubMed: 2017980]
69. McGahan JP. Sonography of the fetal heart: findings on the four-chamber view. AJR Am J Roentgenol. 1991; 156:547–553. [PubMed: 1899755]
70. Shultz SM, Pretorius DH, Budorick NE. Four-chamber view of the fetal heart: demonstration related to menstrual age. J Ultrasound Med. 1994; 13:285–289. [PubMed: 7932993]
71. American Institute of Ultrasound in Medicine. AIUM practice guideline for the performance of obstetric ultrasound examinations. J Ultrasound Med. 2010; 29:157–166. [PubMed: 20040792]
72. American College of Obstetricians and Gynecologists. ACOG Practice Bulletin. Vol. 101. Washington, DC: ACOG; 2009. Ultrasonography in pregnancy.
73. American College of Radiology. Practice guideline for the performance of obstetrical ultrasound. ACR. Revised 2007 (Resolution 25).
74. DeVore GR, Polanco B, Sklansky MS, Platt LD. The 'spin' technique: a new method for examination of the fetal outflow tracts using three-dimensional ultrasound. Ultrasound Obstet Gynecol. 2004; 24:72–82. [PubMed: 15229920]
75. Espinoza J, Kusanovic JP, Goncalves LF, Nien JK, Hassan S, Lee W, Romero R. A novel algorithm for comprehensive fetal echocardiography using 4-dimensional ultrasonography and tomographic imaging. J Ultrasound Med. 2006; 25:947–956. [PubMed: 16870887]

76. Abuhamad A. Automated multiplanar imaging: a novel approach to ultrasonography. J Ultrasound Med. 2004; 23:573–576. [PubMed: 15154522]

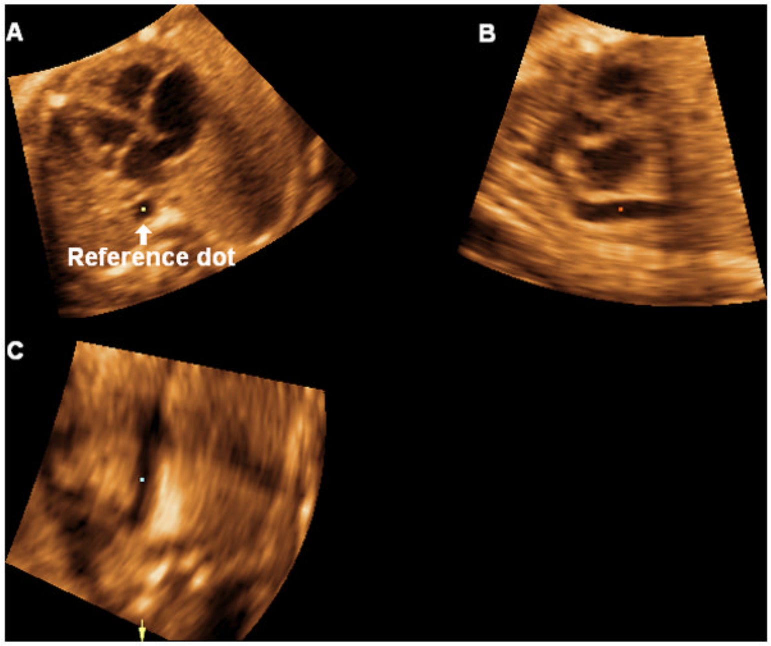

Figure 1.
Volume datasets are adjusted to display the apical four-chamber view in panel A, where the cross-section of the aorta is aligned with the crux of the heart (6 o’clock). The left ventricle is always oriented towards the left side of the image. The reference dot is positioned in the lumen of the aorta, and this allows visualization of a coronal view of the descending aorta in panel C.

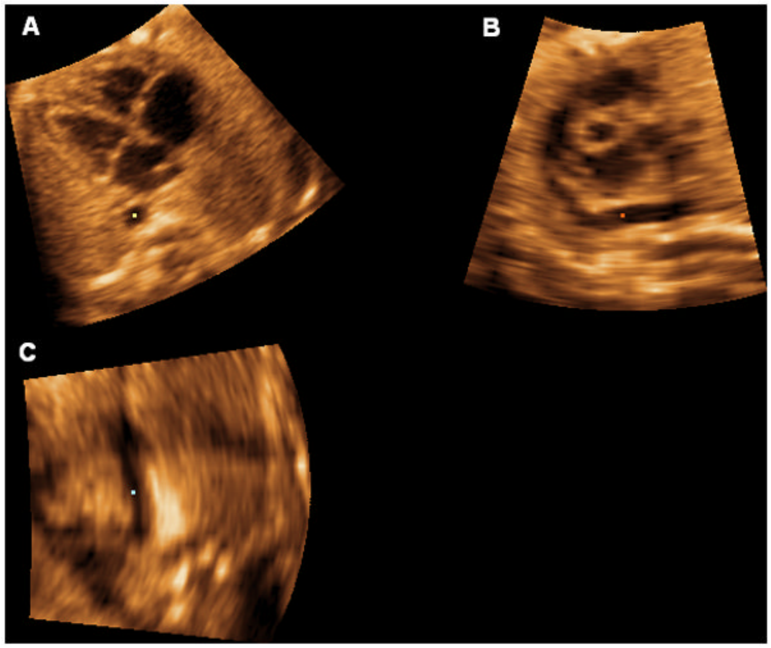

Figure 2.
The image is rotated in panel C so that the aorta is imaged in a vertical or semi-vertical position in order to visualize the longitudinal view of the ductal arch in panel B.

NIH-PA Author Manuscript

NIH-PA Author Manuscript

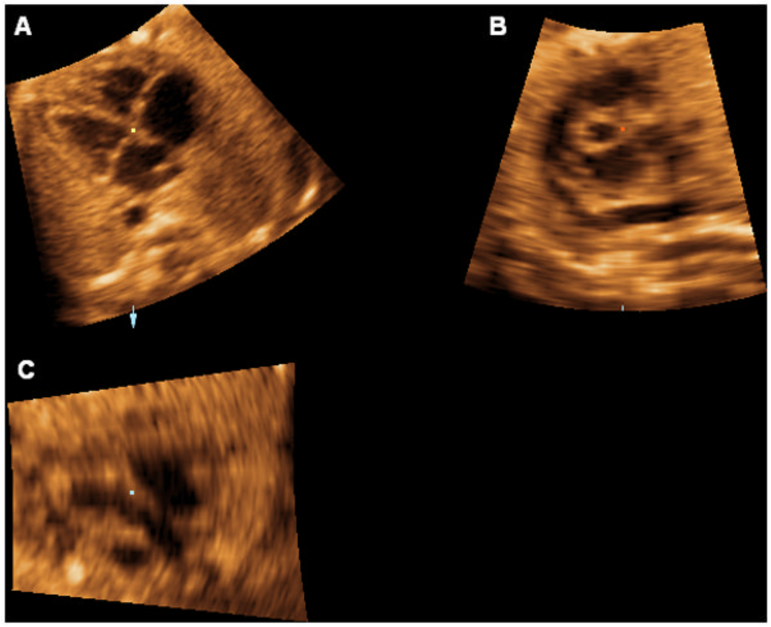

Figure 3.
The reference dot is placed in the crux of the heart (panel A).

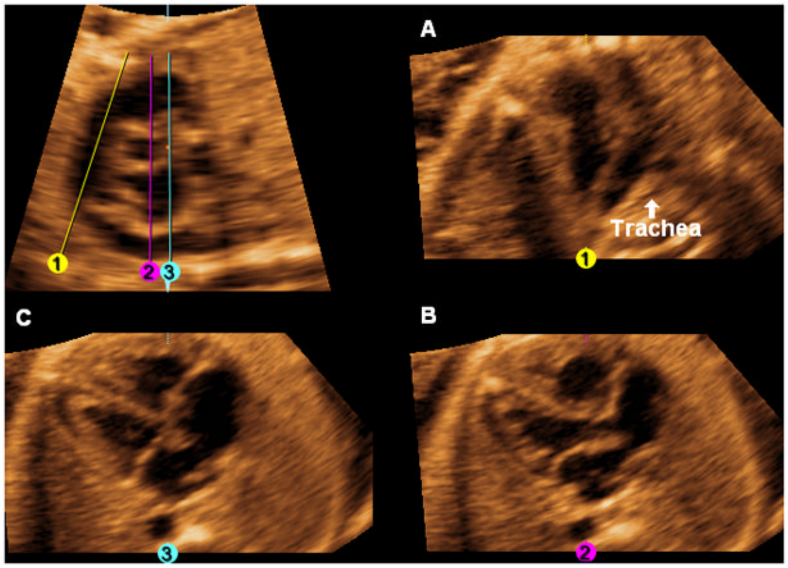

Figure 4.

After activating the OmniView option, the following images are generated by drawing three lines through the longitudinal view of the ductal arch image from top to bottom. **A. Three-vessels and trachea view:** Line 1 (yellow) is a diagonal line drawn through the center of the pulmonary artery parallel to and equidistant from the walls, until it reaches the level of the descending aorta or below. Once Line 1 is completed, it is locked into place by clicking the mouse. The pulmonary artery, aorta, superior vena cava, and trachea are visualized. **B. Five-chamber view:** Line 2 (fuchsia) is a vertical line (6 o'clock) drawn through the right ventricle, center of the aorta (cross-section), left atrium, and descending aorta. Once Line 2 is completed, it is locked into place by clicking the mouse. **C. Four-chamber view:** Line 3 (turquoise) is a vertical line (6 o'clock) drawn through the right ventricle, right external edge of the aorta (cross-section), left atrium, and descending aorta. Once Line 3 is completed, it is locked into place by clicking the mouse. When the three lines are completed, the three-vessels and trachea view, five-chamber view, and four-chamber view will be simultaneously visualized (along with the original longitudinal view of the ductal arch/pulmonary artery).

NIH-PA Author Manuscript
NIH-PA Author Manuscript

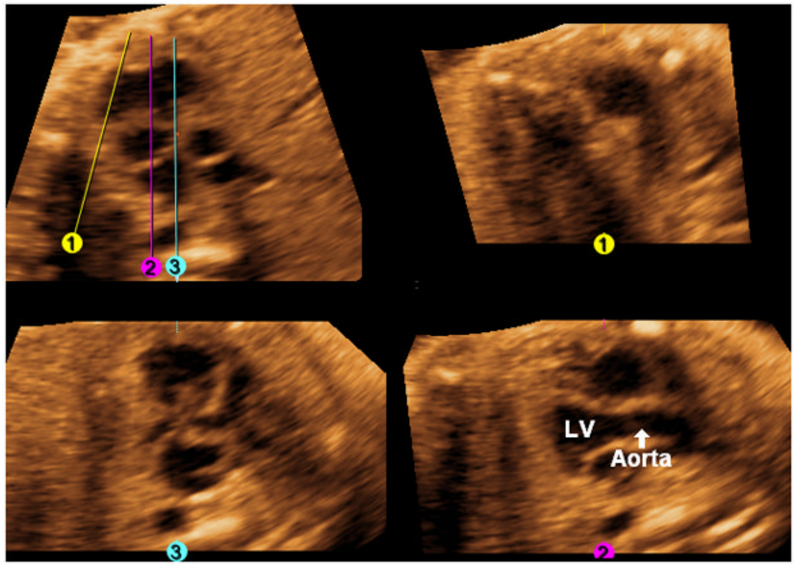

Figure 5. Long axis view of the aorta

The rotation Y option is selected by clicking on the bar, and the five-chamber view is rotated by scrolling on the y-axis (to the right) until the long axis view of the aorta is visualized. A scroll on the y-axis (back to the left) is performed until the original views (three-vessels and trachea view, five-chamber view, four-chamber view) are again simultaneously visualized (not shown). The next step will be performance of the “swing technique”. LV, left ventricle.

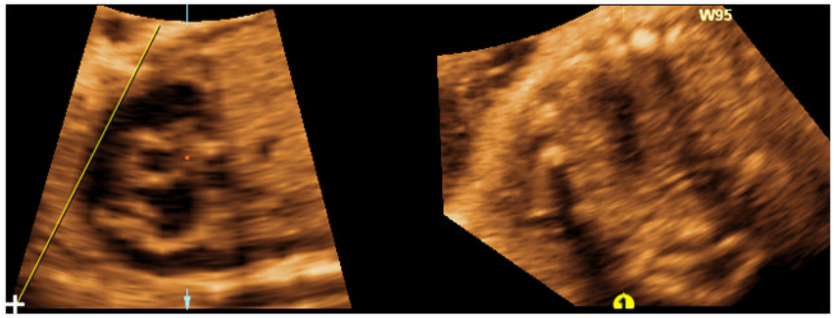

Figure 6. " Swing technique" (placement of "swing" line)

At the top of the longitudinal view of the ductal arch image, the "swing" line is begun approximately above the center of the right ventricle and is *fixed (but not locked)* on this end only. The line is drawn from the top to the lower left hand corner of the image, making sure it is lateral to the ductal arch. The line should remain *unlocked* with the cursor (not the "lollipop") visualized at its inferior end.

NIH-PA Author Manuscript

NIH-PA Author Manuscript

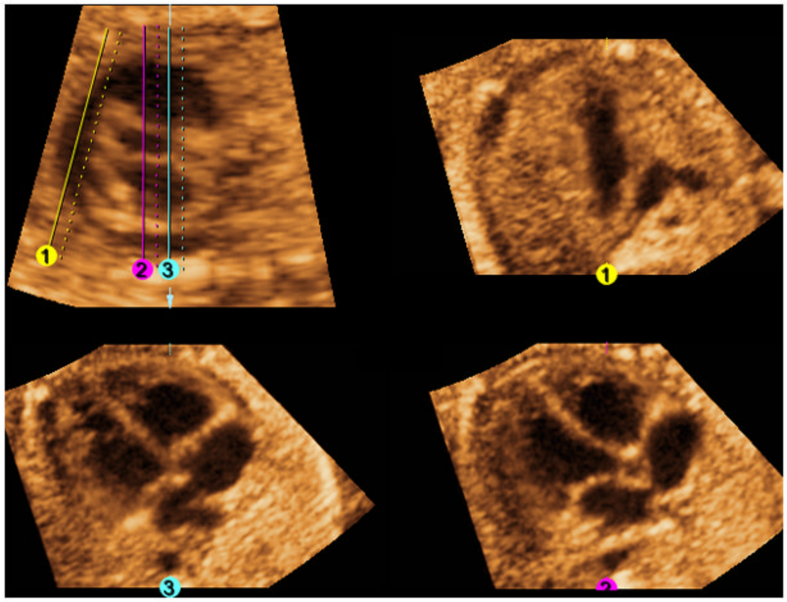

Figure 7. FAST Echo algorithm and Volume Contrast Imaging (VCI) applied to a normal fetus at 26 weeks of gestation

All three independent planes are simultaneously visualized (along with the longitudinal view of the ductal arch/pulmonary artery) after placement of 3 lines. VCI has been activated with a slice thickness of 2 mm and X-ray/surface smooth (Mix 100/0%) render mode applied. VCI allows images to appear smoother and the interface between different tissues to be more apparent. The render direction applies from the solid to the dotted line.

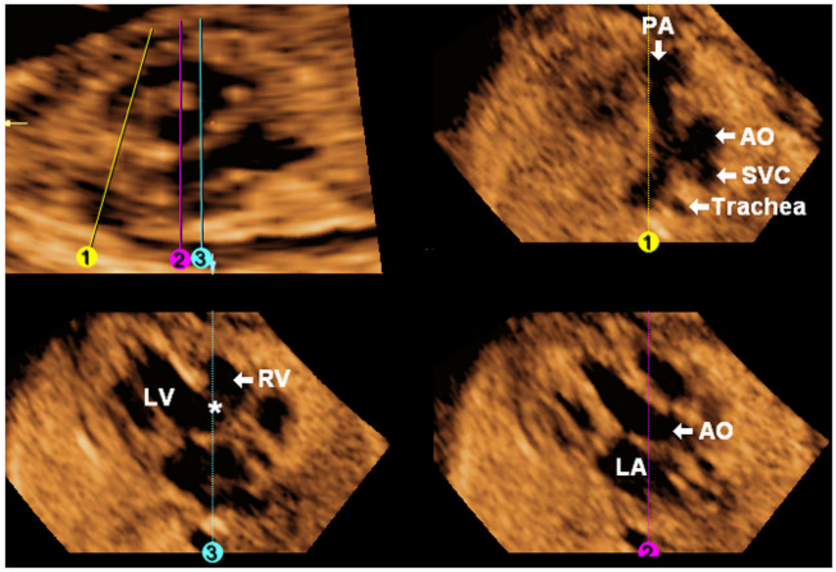

Figure 8. FAST Echo algorithm applied to a fetus with tricuspid atresia and ventricular septal defect (hypoplastic right ventricle) at 21 weeks of gestation

The longitudinal view of the ductal arch appears abnormal, and both this view and the three-vessels and trachea view (Line 1) show a small pulmonary artery, consistent with pulmonic stenosis. Placement of Line 2 shows the aorta arising from the left ventricle. The four chamber view is abnormal (Line 3) with a large ventricular septal defect (asterisk), and a hypoplastic right ventricle. AO, aorta; LA, left atrium; LV, left ventricle; PA, pulmonary artery; RV, right ventricle; SVC, superior vena cava.

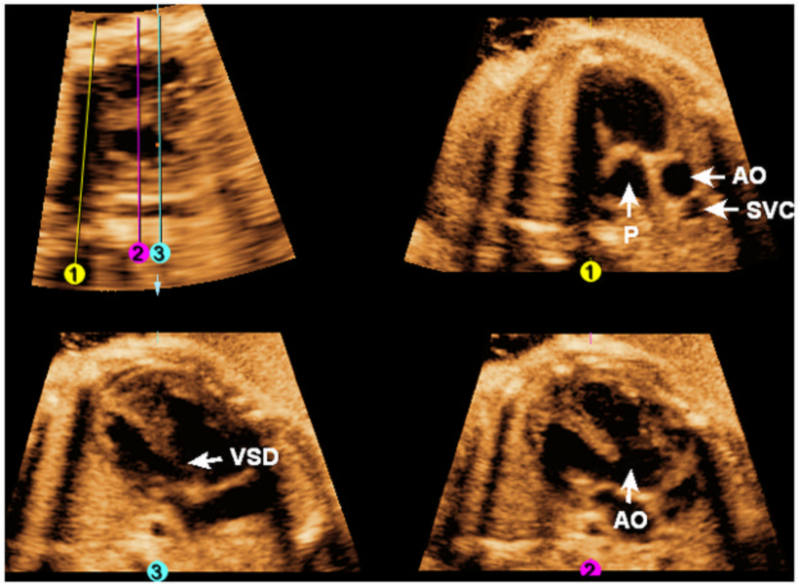

Figure 9. FAST Echo algorithm applied to a fetus with tetralogy of Fallot at 33 weeks of gestation

Placement of Line 1 shows evidence of pulmonic stenosis with an abnormally thickened valve. Placement of Line 2 shows the overriding aorta. Placement of Line 3 shows an abnormal four-chamber view with a large ventricular septal defect. AO, aorta; P, pulmonary artery; SVC, superior vena cava; VSD, ventricular septal defect.

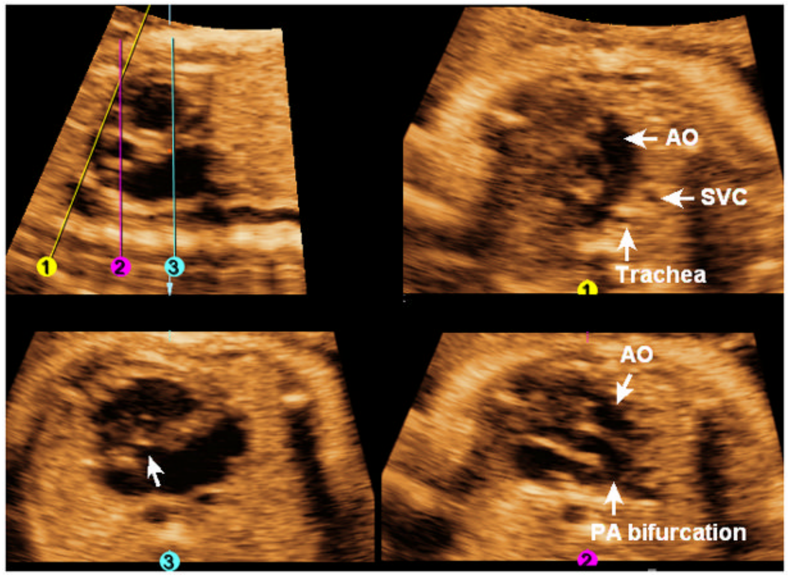

Figure 10. FAST Echo algorithm applied to a fetus with complete atrioventricular canal defect and transposition of great vessels at 30 weeks of gestation

In the longitudinal view of the ductal arch, the descending aorta is visualized, but not the pulmonary artery. The three-vessels and trachea view (line 1) is abnormal, and shows the aorta, superior vena cava, and trachea; however the pulmonary artery is not visualized. In the five-chamber view (Line 2), the aorta is visualized anteriorly, while the pulmonary artery (confirmed by its bifurcation) arises leftward from the common ventricular chamber. The four-chamber view (Line 3) shows a common atrioventricular valve (arrow) and a large septal defect involving both the atrial and ventricular septa. AO, aorta; PA, pulmonary artery; SVC, superior vena cava.

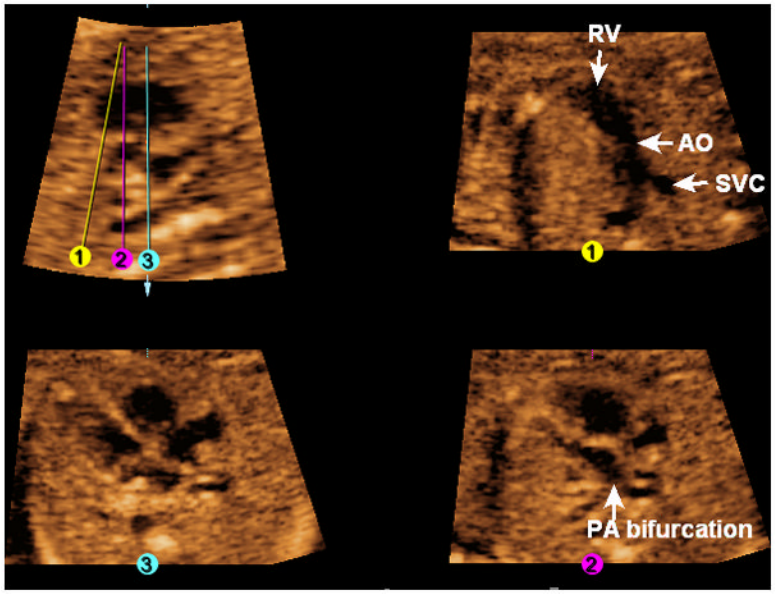

Figure 11. FAST Echo algorithm applied to a fetus with transposition of great vessels at 20 weeks of gestation

The four-chamber view appears normal (Line 3). In the longitudinal view of the ductal arch, the pulmonary artery and ductus arteriosus are not visualized. The three-vessels and trachea view (Line 1) is abnormal, and shows only the aorta (arising from the right ventricle) and superior vena cava. After placement of Line 2, the pulmonary artery (confirmed by its bifurcation) is seen exiting the left ventricle. AO, aorta; PA, pulmonary artery; RV, right ventricle; SVC, superior vena cava.

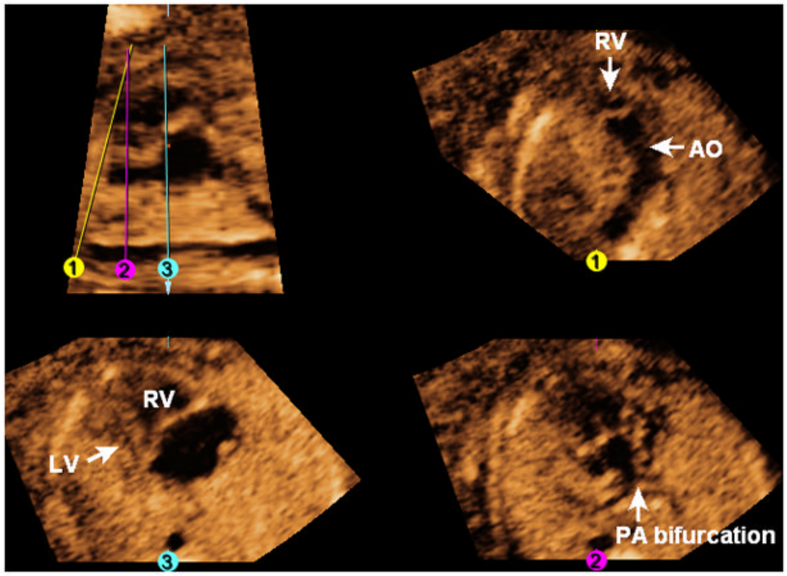

Figure 12. FAST Echo algorithm applied to a fetus with hypoplastic left heart, double outlet right ventricle, transposition of great vessels, and heterotaxy at 19 weeks of gestation

In the longitudinal view of the ductal arch, the descending aorta is visualized, but the pulmonary artery and ductus arteriosus are not seen. The three-vessels and trachea view (Line 1) is abnormal, and shows the aorta arising from the right ventricle. After placement of Line 2, the pulmonary artery (confirmed by its bifurcation) is seen to exit leftwards from the right ventricle. The four-chamber view (Line 3) shows the hypoplastic left heart. AO, aorta; LV, left ventricle; PA, pulmonary artery; RV, right ventricle.